

<sup>1</sup> Combining individual and close-kin mark-recapture to design  
<sup>2</sup> an effective wildlife population survey

<sup>3</sup> Eiren K. Jacobson<sup>1\*</sup>, Mark V. Bravington<sup>2</sup>, Rebecca L. Taylor<sup>3</sup>,  
Irina S. Trukhanova<sup>4,5</sup>, David L. Miller<sup>6</sup>, William S. Beatty<sup>7</sup>

<sup>4</sup> 10th February 2026

<sup>5</sup> <sup>1</sup> Centre for Research into Ecological & Environmental Modelling and School of Mathematics &  
<sup>6</sup> Statistics, University of St Andrews, St Andrews, Scotland

<sup>7</sup> <sup>2</sup> Estimark Research, Hobart, Australia

<sup>8</sup> <sup>3</sup> US Geological Survey, Alaska Science Center, Anchorage, Alaska

<sup>9</sup> <sup>4</sup> North Pacific Wildlife Consulting, LLC, Seattle, Washington

<sup>10</sup> <sup>5</sup> US Fish and Wildlife Service, Marine Mammals Management, Anchorage, Alaska

<sup>11</sup> <sup>6</sup> Independent Researcher, Dundee, Scotland

<sup>12</sup> <sup>7</sup> US Geological Survey, Upper Midwest Environmental Sciences Center, La Crosse, Wisconsin

<sup>13</sup> \*Corresponding author email: ej45@st-andrews.ac.uk

<sup>14</sup> **Journal Name:** Ecology

<sup>15</sup> **Manuscript Type:** Article

<sup>16</sup> **Open Research Statement:** Code to reproduce the analyses presented in this manuscript is available  
<sup>17</sup> at [https://www.github.com/eirenjacobsen/JacobsonEtAl\\_WalrusCKMR\\_Ecology](https://www.github.com/eirenjacobsen/JacobsonEtAl_WalrusCKMR_Ecology). No data were  
<sup>18</sup> collected for this study.

<sup>19</sup> **Keywords:** close-kin mark-recapture, individual genetic mark-recapture, survey design, walrus

## Abstract

Close-kin mark-recapture (CKMR) is a promising approach for assessing population size of species which have been difficult to survey using more traditional methods. Here, we combine individual and close-kin mark-recapture in a single modelling framework (ICKMR) and provide an example of study design using this approach for Pacific walrus (*Odobenus rosmarus divergens*). We develop the ICKMR model and test it using simulated datasets, then use properties of the pseudo-likelihood to investigate the expected precision in estimates of abundance with different proposed survey designs. Our motivating example, the Pacific walrus, is an ice-associated marine mammal found in the Bering and Chukchi seas, where it is an important resource for Indigenous peoples. Pacific walrus abundance declined in the late 20th century, and it is currently a species of conservation concern due to potential impacts of climate change, particularly the loss of sea ice. To reduce uncertainty in population size estimates, researchers undertook a genetic mark-recapture sampling campaign from 2013-2017 and collected tissue samples from over 8,000 individuals. Another campaign of a similar scale is ongoing (2023-2028). While sample collection was designed for individual mark-recapture, advances in CKMR methods and associated molecular techniques mean that these samples could also be suitable for CKMR. The advantages of CKMR over mark-recapture include an increased effective sample size (because each individual tags itself and its parents, siblings, and offspring) and additional insights into demographic quantities of interest. To make best use of genetic samples, we combine individual mark-recapture (IMR) with CKMR (ICKMR) and investigate whether different sampling strategies can increase precision in estimates of abundance. Our modeling approach includes special considerations for walrus life-history, including a multi-year inter-birth interval. We found that expected CVs of the ICKMR estimates of abundance, adult female survival, juvenile female survival, and proportion of breeding females are lower than those expected from IMR alone, and with ICKMR, fewer years of future sampling can be conducted to obtain sufficient precision in estimates of abundance. This work demonstrates the utility of ICKMR and could be applicable across a variety of taxa.

## 46 1 Introduction

47 Estimation of abundance and other demographic parameters such as survival are a key part of wildlife  
48 management and conservation. Traditional mark-recapture analysis (Williams et al., 2002) can deliver  
49 estimates with low bias and uncertainty, provided enough individual animals (*i*) are identifiable by  
50 natural, artificial, or genetic “marks” and (*ii*) can be recaptured over time. If genotypes are used  
51 as marks, as in genetic individual mark-recapture (IMR; Palsbøll et al., 1997), then kinship patterns  
52 amongst samples (e.g., parents, siblings) contain additional demographic information (Skaug, 2001).  
53 Close-kin mark-recapture (CKMR; refer to Bravington et al., 2016) is a framework for using pairwise  
54 kinships, as inferred from genotypes, to estimate abundance and demographic parameters. CKMR  
55 provides additional flexibility compared to IMR because it is not essential to recapture individuals, so  
56 lethal (e.g., from sampling, harvest, or natural mortality) and/or non-lethal samples can be used. As  
57 of 2025, most CKMR projects have focused on commercial fish (e.g., Davies et al., 2020) or sharks  
58 (e.g., Hillary et al., 2018), but a few have been conducted on mammals (e.g., Conn et al., 2020; Taras  
59 et al., 2024; Lloyd-Jones et al., 2023).

60 The principle behind CKMR is that every individual has one mother and one father, so each  
61 captured individual “tags” itself and its parents. For a given sample size, a large population is expected  
62 to have fewer “recaptures” of closely related individuals compared to a small population. In practice,  
63 CKMR data are derived from pairwise comparisons among samples while considering covariates such  
64 as age, size, and sex. Each pair of samples is tested for a series of kinship relationships such as parent-  
65 offspring, half-sibling, or self (the alternative being “unrelated”, i.e., none of the above). The CKMR  
66 model has two components: (*i*) a population-dynamics model driven by the demographic parameters;  
67 and (*ii*) formulae for expected frequencies of different kinship types in pairwise comparisons that are  
68 conditional on sample covariates and demographic parameters. By combining the kinship data with  
69 the population dynamics model, parameters can be estimated using maximum likelihood or Bayesian  
70 methods.

71 The success of CKMR depends on whether the data collected contain enough close-kin pairs to  
72 yield acceptable precision in parameter estimates. The chance of success is greatly increased by a  
73 study design exercise that evaluates the effects of sample age, size, and sex composition of sampled  
74 animals, precision of covariate measurements, and study duration, while taking into account the species’  
75 life history, ecology, and physiology (Sévèque et al., 2024; Petersma et al., 2024; Merriell et al., 2024;  
76 Swenson et al., 2024; Waples and Feutry, 2022). The pairwise comparison framework leads to analytical

77 results for the expected number of kin pairs and the parameter-estimation variance, given the number  
78 of samples and associated covariates, so that simulation is not essential for study design. Nevertheless,  
79 simulation can be used to check kinship probability formulae, robustness to model simplifications, and  
80 design setup.

81 In this study, we perform and verify CKMR design calculations for the Pacific walrus (*Odobenus*  
82 *rosmarus divergens*; hereafter, walrus), to demonstrate the design process and the utility of CKMR.  
83 Our goal was to understand how different possible demographic scenarios and design choices would  
84 impact precision of estimates of adult female abundance, adult female survival, and juvenile survival.  
85 In addition, in most CKMR applications to date, self-recaptures were unlikely or impossible (e.g.,  
86 when sampling is lethal). Lloyd-Jones et al. (2023) included IMR results in a CKMR study but did  
87 not integrate both datasets into a single model. Bravington et al. (2014) extended CKMR to include  
88 IMR as an additional kinship type (ICKMR), whereby pairwise genetic comparisons can show that  
89 two samples are from the same animal. They found that the expected CV in estimates of abundance  
90 decreased from approximately 30% with IMR alone to approximately 20% with ICKMR. Here, we  
91 explore design scenarios using IMR alone versus a combined ICKMR approach, and we find that the  
92 latter can be used to reduce the amount of survey effort required for adequate monitoring.

### 93 1.1 Pacific walrus biology and background

94 The Pacific walrus is a gregarious, ice-associated pinniped inhabiting continental shelf waters of the  
95 Bering and Chukchi seas. During winter (when sea ice forms south of the Bering Strait), almost all  
96 walruses occupy the Bering Sea (Fay, 1982). In summer (when sea ice is absent from the Bering Sea)  
97 almost all juvenile and adult female walruses, and some adult male walruses, migrate north to the  
98 Chukchi Sea. When walruses rest offshore on sea-ice floes, their distribution is dynamic because it  
99 generally follows the marginal ice zone, which is a moving, changing habitat which contains a mix  
100 of ice floes and open water). Pacific walruses are considered a single, panmictic population (Beatty  
101 et al., 2020) and are managed as a single stock (US Fish and Wildlife Service, 2023). Adult female  
102 walruses move between US and Russian waters of the Chukchi Sea over the course of a single season  
103 (Jay et al., 2012; Udevitz et al., 2017). Female walruses breed in winter and give birth to a single  
104 calf approximately 14-15 months later (Fay, 1982; Robeck et al., 2022). Mothers and calves maintain  
105 a close physical relationship for the first year, and weaning generally occurs between the first and  
106 second year (Fay, 1982), though juveniles may travel with their mother until 3 years of age (Beatty

107 et al., 2020). Female walruses may have their first calf at 6 years of age; male walruses do not reach  
108 sexual maturity until 15 years of age (Fay, 1985). Maximum walrus lifespan is approximately 40 years  
109 (Fay, 1982). Walruses can be aged from their teeth (Kryukova, 2014) and work is ongoing to develop  
110 an epigenetic clock for walrus biopsy samples (i.e., estimated ages within 10% of true values; Robeck  
111 et al., 2023a).

112 Abundance and demographic rate estimates are crucial for understanding population status and  
113 trends, as well as for co-developing harvest management plans. Continued sea-ice loss and a con-  
114 comitant increase in the intensity and expansion of industrial and shipping activities in Pacific Arctic  
115 waters (Silber and Adams, 2019) are expected to drive a substantial population decline (US Fish and  
116 Wildlife Service, 2011; MacCracken et al., 2017; Johnson et al., 2024a; Johnson et al., 2024b). Sub-  
117 sistence walrus harvests in Alaska and Chukotka exceed 4,000 animals annually (US Fish and Wildlife  
118 Service, 2023), and Indigenous peoples and co-management agencies need information on the status of  
119 the walrus population to manage these harvests sustainably. Furthermore, in the United States, the  
120 Marine Mammal Protection Act (MMPA; P.L. 92-522; 16 U.S.C. §§1361-1423h) requires a determina-  
121 tion of potential biological removal for walruses, which, in turn, requires a precise abundance estimate  
122 (Gilbert, 1999; Wade and DeMaster, 1999).

123 Scientists have attempted to ascertain walrus population size since at least 1880 (Fay et al., 1989),  
124 and until very recently, the most concerted effort was the 1975-2006 range-wide aerial surveys conducted  
125 collaboratively by the USA and the USSR and, later, the Russian Federation. However, abundance  
126 estimates from these surveys were biased and imprecise. Aerial surveys were abandoned after the  
127 2006 survey which yielded a 95% confidence interval (CI) of 55,000–507,000 animals and coefficient  
128 of variation (CV) of 0.93 for the population abundance estimate of 129,000 despite a rigorous design,  
129 innovative field methods, and sophisticated analyses. The imprecision in the estimate resulted from  
130 the walrus population being widely dispersed with unpredictable local clumping (Speckman et al.,  
131 2011; Jay et al., 2012). The first rigorous walrus survival rate estimates were obtained within the past  
132 decade via Bayesian integrated population models (IPMs), which combined multiple data sources to  
133 estimate demographic rates and population trends over multiple decades (Taylor and Udevitz, 2015;  
134 Taylor et al., 2018). However, problems with the aerial survey data continued to preclude conclusions  
135 about population abundance in the IPMs (Taylor and Udevitz, 2015).

136 In 2013, the US Fish and Wildlife Service (FWS) began a genetic IMR project to estimate walrus  
137 abundance and demographic rates (Beatty et al., 2020; Beatty et al., 2022). Genetic “marking” via skin

138 biopsy samples (Palsbøll et al., 1997) is preferable to traditional marking techniques because walruses  
139 are extremely difficult to handle physically. In five summer research expeditions, biologists tried to  
140 biopsy a representative sample of walruses. In 2013, 2014, and 2016, biopsy samples were collected in  
141 US waters; in 2015 and 2017, biopsy samples were collected in both US and Russian waters (Beatty  
142 et al., 2022). Sampling focused on groups of adult females and juveniles because these classes are the  
143 demographically important population segments of this polygynous species (Fay, 1982; Beatty et al.,  
144 2022). Further details are given in Beatty et al. (2020) and Beatty et al. (2022). Data analysis from the  
145 2013–2017 expeditions used a Cormack-Jolly-Seber multievent model to estimate survival rates, and a  
146 Horvitz-Thompson-like estimator to obtain population size. The total abundance estimate of 257,000  
147 had a 95% credible interval (CrI) of 171,000–366,000 (CV=0.19; Beatty et al. 2022). Although this  
148 was more precise than historical estimates from surveys (e.g., Speckman et al., 2011), the IMR study  
149 required extensive investment of human and financial resources. Thus, FWS and the US Geological  
150 Survey (USGS) initiated a second generation of expeditions in 2023 to estimate walrus abundance and  
151 vital rates with CKMR. Initially, expeditions were planned to occur each June from 2023-2027. A  
152 successful expedition to collect biopsy samples and other data was completed in 2023, but no samples  
153 were collected in 2024. Here we explore ICKMR as a way to substantially increase the information  
154 content of IMR without increasing sampling effort.

## 155 2 Methods

156 Our methods consist of two main components: (2.1) ICKMR model development and (2.2) simulation  
157 for model checking and design scenarios. To develop the ICKMR model, we (2.1.1) selected the kinship  
158 categories that should be common in the samples as well as informative about recent abundance,  
159 (2.1.2) built a walrus-specific population dynamics model capable of handling those kinships, (2.1.3)  
160 formulated pairwise kinship probabilities, (2.1.4) defined the pseudo-likelihood, and (2.1.5) performed  
161 design calculations. We then (2.2.1) developed an individual-based simulation with walrus life history,  
162 (2.2.2) used this simulation to check our ICKMR model, and (2.2.3) generated simulated datasets from  
163 different demographic scenarios of interest with which we evaluated expected precision in parameter  
164 estimates under different possible survey designs.

165 **2.1 ICKMR model development**

166 **2.1.1 Kinship Types**

167 First, we considered which types of kinship may occur and are possible to detect in the population of  
168 interest given our knowledge of life history, resolution of genetic methods, and survey design. CKMR  
169 datasets often contain multiple genetically detectable kinships, all potentially providing some infor-  
170 mation about population dynamics. Potential kinships fall into three basic categories (though refer  
171 to Discussion): parent-offspring pairs (POPs); full-sibling pairs (FSPs); and second-order kin pairs  
172 (2KPs, comprising half-sibling pairs (HSPs), grandparent-grandchild pairs (GGPs), and full-thiatic  
173 pairs (FTP), such as aunt-nephew). Not all those possible kinships would be informative about the  
174 most important aspects of walrus dynamics: abundance, trend, and mortality.

175 We ignored paternal HSPs and father-offspring pairs (FOPs) and did not model male adults at  
176 all because of irresolvable confounding between adult male abundance and persistent variability in  
177 breeding success (which is likely given lek-based breeding; refer to Appendix S1: Section S1 for more  
178 details). We did not include within-cohort HSPs or FSPs because walruses have a litter size of one and  
179 female walruses are unlikely to repeatedly mate with the same male. Similarly, we did not consider  
180 FTPs. GGPs are difficult to distinguish from HSPs, but we assume that they would be rare in our  
181 survey sample and could be excluded (refer to Appendix S1: Section S2). We are thus left with three  
182 kinships: mother-offspring pairs (MOPs), maternal half-sibling pairs (XmHSPs), and self-pairs (SPs)  
183 where an individual is captured at least twice and in different years. Note that male juvenile samples,  
184 which are common, are used as potential offspring or XmHSPs (i.e., they mark their mothers), but  
185 not as potential SPs or fathers. For model development and design, we assume that all kinship types  
186 are detected accurately.

187 **2.1.2 Life history and population dynamics**

188 **Stage-structured quasi-equilibrium dynamics** In order to formulate kinship probability equa-  
189 tions, CKMR requires a population dynamics model. In this case, we only needed to model females. We  
190 used a stage-structured (juvenile/adult), rather than fully-age-structured approach because (i) most  
191 reproductive female adults are expected to have similar reproductive capacity and chance of survival  
192 and (ii) stage-structured models are simpler to implement for CKMR and require fewer parameters.  
193 Given these factors, and the broad goal of estimating female adult abundance, a stage-structured  
194 model should be adequate for design purposes. We also opted not to include calves in the model

195 because early-life-history survival (before animals are easily sampled) would require extra parameters  
196 that are difficult to estimate directly. In effect, calf survival and birth rate are combined into overall  
197 rate-of-change in abundance, which becomes a single parameter to be estimated.

198 The parameters to be estimated were adult female and juvenile female survival rates ( $\phi_A$  and  $\phi_J$ ),  
199 adult female abundance in some reference year ( $N_{y,A}$ ), and population trend ( $r$ ). We used two stages:  
200 juveniles aged 1–5, and adults aged 6+ (the first age at which an accompanying calf is common). We  
201 assumed constant survival within each stage ( $\phi_A$  and  $\phi_J$ ). Because weaning occurs between 1 and 2  
202 years of age (Fay, 1982) and most adult female mortality occurs during the subsistence harvest in the  
203 spring when 1-yr-old walruses are nearly 2, we assumed that offspring survival from age 1 onwards was  
204 independent of its mother’s survival. This is consistent with Taylor et al. (2018). While we assume  
205 that offspring survival is independent from age 1, we do not assume that sampling is independent until  
206 age 6 (refer to Section 2.1.3). Our model assumed that adult female abundance increased or decreased  
207 exponentially over the period covered by the population dynamics, which we set at 2000–2028. The  
208 model needs to cover all birth dates of samples that are used as potential offspring, XmHSPs, or  
209 SPs; choosing a lower limit of 2000 thus discards a few samples, but because there was more intense  
210 harvesting prior to 2000 and large changes in abundance (Taylor and Udevitz, 2015; Taylor et al.,  
211 2018) pre-2000 age composition is difficult to model.

212 Adult female abundance in year  $y$  ( $N_{y,A}$ ) is described by

$$N_{y,A} = N_{y_0,A} e^{r(y-y_0)} \quad (1)$$

213 where  $e^r$  is the rate of population change and  $r = 0$  corresponds to stasis.

214 To incorporate self-recaptures in the close-kin model, we must assume stable age composition  
215 within stage. For that purpose, we assume that age composition over the modeled period is adequately  
216 described by the stable-age or “quasi-equilibrium” distribution consistent with survival  $\phi_A$  and rate of  
217 change  $e^r$ . As shown in e.g., Keyfitz and Caswell (2005) Chapter 5, this is  $N_{y,a} \propto N_{y,A} \phi_A^a e^{-ra}$ .

218 **The breeding cycle** Female walruses, like many other animals, exhibit “skip-breeding”, taking gaps  
219 of one or more years between births. This intermittent breeding can cause bias in parameter estimates  
220 if not included in the CKMR model (Waples and Feutry, 2022; Swenson et al., 2024). Because XmHSPs  
221 will be important for walruses, we decided to include a sub-model for skip-breeding with parameters  
222 to be estimated from the CKMR data.

223 Walruses have a litter size of one, and due to a 14-15 month gestation, they cannot give birth in  
 224 consecutive years (Fay, 1982; Katsumata et al., 2020; Robeck et al., 2022). They are also unlikely to  
 225 give birth every second year (Taylor and Udevitz, 2015; Fay et al., 1997; Taylor et al., 2018; Robeck  
 226 et al., 2023a). We used a first-order Markov model to describe the walrus breeding cycle (Fig. 1).  
 227 We assume three breeding states: (S1) pregnant; (S2) with young-of-the-year (YOTY) calf; or (S3)  
 228 mature and not in S1 or S2. From state S1 (pregnant), next year's state must be S2 (with YOTY  
 229 calf). From state S2, a female may next year either return to state S1 (become pregnant again), with  
 230 probability  $\psi_2$ , or move to state S3 (quiescent: neither pregnant nor with calf) with probability  $1 - \psi_2$ .  
 231 From state S3, she will either move to state S1 (become pregnant) with probability  $\psi_3$ , or remain in  
 232 state S3 with probability  $1 - \psi_3$ .

233 Females enter the breeding cycle at state S3 (i.e., reach sexual maturity) at age 4, and therefore  
 234 sometimes become pregnant at age 5 and give birth at age 6 (Fay, 1982). Depending on the values of  
 235  $\psi_2$  and  $\psi_3$ , this leads to fluctuations in effective fecundity (i.e., probability of being in state S2) over the  
 236 first few years of adult life. Both  $\psi_2$  and  $\psi_3$  are estimated within the CKMR model, ultimately based on  
 237 the observed distribution of birth gaps between XmHSPs. We do not use any data on whether females  
 238 were with or without calf when sampled, and we cannot distinguish between fine-scale aspects of the  
 239 reproductive cycle, such as differences in fertilization/implantation rates versus pregnancy failures or  
 240 neonatal deaths. Thus, because the transition from S1 (pregnant) to S2 (with YOTY calf) is set to 1,  
 241 reproductive failures are subsumed by the fecundity rate.

242 We later use two quantities derived from the breeding cycle. First, we calculated the (average)  
 243 proportion of adult females in S2 (with YOTY),  $\bar{\beta}_2$ . Let  $\Psi$  be the  $(3 \times 3)$  transition matrix implied by  
 244 the breeding cycle (Fig. 1). Taking the eigendecomposition of  $\Psi$ , we extracted the second element of  
 245 the eigenvector with the largest eigenvalue to obtain  $\bar{\beta}_2$  (Caswell, 2001). Second, we defined fecundity  
 246 as a function of age  $B(a)$ , where the numerator in Eq. 2 gives the probability that any female of age  
 247  $a$  is in state S2. Thus,

$$F(a) \triangleq \frac{\mathbb{P}[B(a) = 2]}{\bar{\beta}_2}, \quad (2)$$

248 immature animals have fecundity 0, and an average adult has fecundity 1.

249 **2.1.3 Kinship probabilities**

250 Having formulated our population dynamics model, we now quantify the probability of relatedness  
251 between individuals. These probabilities will be used in the pairwise comparison terms summed in the  
252 pseudo-log-likelihood. The kinship probabilities are linked to the population dynamics model by shared  
253 parameters. For walruses, we considered three types of kinship: mother-offspring pair (MOP), cross-  
254 cohort maternal half-sibling pair (XmHSP), and self-pair (SP), which represents individual recaptures  
255 in different years.

256 To establish demographic kinship probabilities between two sampled individuals, we apply the  
257 principle of expected relative reproductive output (ERRO; Bravington et al., 2016). For example, the  
258 probability that a given adult female is the parent of an independently sampled offspring is the ratio  
259 of that adult's expected fecundity to the total fecundity of all parents at the time the offspring was  
260 born. We denote the kinship for individuals  $i$  and  $j$  as  $K_{ij}$ , which in our case may be MOP, XmHSP,  
261 SP, or unrelated pair (UP). Sampling was assumed to occur on an annual basis, i.e., a maximum of one  
262 sample per individual per year would be used and any within-year individual recaptures discarded. In  
263 the case of MOPs and XmHSPs, if recaptures exist in different years, we ensure that only one sample  
264 (the last) from each individual is used (so “sample” and “individual” are interchangeable terms). We  
265 can then be certain that the individual was alive until the time of the last sample, and so, conditional  
266 on age, could have produced offspring at least up until that time. In addition, using only the last  
267 sample improves precision in estimates of survival because the individual definitely survived to age  
268 at last sample. For SPs, we consider the first and last sample from each individual (in which case,  
269 “sample” and “individual” have different meanings) to maximize the interval over which we can be  
270 certain that the individual was alive.

271 We use the following notation: individual  $i$ , sampled at age  $a_i$  in year  $y_i$  with birth year  $b_i \triangleq y_i - a_i$ .  
272 As noted above, we only estimate adult female abundance. However, we use notation that could be  
273 adopted in models that estimate both juvenile and adult female abundance. In our notation,  $N_{y,A}$   
274 refers to adult female abundance in year  $y$ . We include the A subscript for clarity throughout the  
275 manuscript. In our derivation of juvenile female abundance (Appendix S1: Section S3), we simply  
276 change the second subscript to J for juvenile,  $N_{y,J}$ . Thus, we generalize this notation to  $N_{y,d}$  where  
277  $y$  denotes year and  $d$  denotes developmental stage (A = adult or J = juvenile). We define the binary  
278 variable  $L$  to indicate lethality of sampling ( $L_i = 1$  indicates lethal sampling for sample  $i$ ). We use  $\mathbb{I}()$   
279 as an indicator function, returning 1 when the condition inside the brackets is true, else 0. Kinship

280 probabilities are functions of demographic parameters such as  $\phi_A$  and  $N_{y_0, A}$ ; we use  $\theta$  as shorthand for  
 281 this set of parameters, which become explicit in later iterations of the formulae.

282 We assumed that epigenetic age estimates will be available for all samples, based on an epigenetic  
 283 aging approach (Polanowski et al., 2014; Robeck et al., 2023b). Our model could be extended to  
 284 incorporate errors in estimated age (with standard deviation assumed known, i.e., after calibration of  
 285 epigenetic age to known-age samples), though the results here assume no errors; refer to the Discussion  
 286 section.

287 **Mother-offspring pairs (MOPs)** Consider a comparison between a potential mother  $i$ , to a po-  
 288 tential offspring  $j$ . We restrict our analysis to comparisons that satisfy the following:

- 289 •  $i$  is female (though  $j$  need not be);
- 290 •  $a_j \geq 1$  (no YOTY samples are used);
- 291 •  $y_i \neq y_j \vee a_j \geq a_b$  (do not compare potential offspring and mothers sampled in the same year  
 292 unless offspring age is at least the age of first birth,  $a_b = 6$ );
- 293 •  $b_j \geq 2000$  (birth year of potential offspring must be greater than or equal to 2000, because  
 294 population dynamics starts at year 2000).

295 Walruses may accompany their mothers until age 3 (Beatty et al., 2020). To ensure independence, we  
 296 do not compare potential offspring that are juveniles ( $\leq 5$  years old) to potential mothers sampled in  
 297 the same year. However, we do compare potential offspring that are adults ( $\geq 6$  years old) to potential  
 298 mothers sampled in the same year. Furthermore, we compare all potential offspring to all potential  
 299 mothers sampled in different years, regardless of age, because we assume that the sampling events are  
 300 independent.

301 We can now distinguish two cases:  $y_i < b_j$  (potential mother sampled before potential offspring  
 302 birth) and  $y_i \geq b_j$  (potential mother sampled after potential offspring birth).

303 For  $y_i < b_j$ , individual  $i$  still has to survive one or more years in order to be individual  $j$ 's mother  
 304 (note that  $i$  may be immature when sampled, but mature by the time of  $j$ 's birth). In this case  $i$ 's  
 305 sampling *must* be non-lethal ( $L_i = 0$ ). The MOP probability is

$$\mathbb{P}[K_{ij} = \text{MOP} | a_i, y_i, b_j, L_i = 0, \theta] = \frac{R_i(b_j | y_i, a_i)}{R^+(b_j)} \quad (3)$$

306 where  $R_i(b_j|y_i, a_i)$  is the expected reproductive output (ERO) of individual  $i$  in year  $b_j$  given  $i$  is  
 307 age  $a_i$  in year  $y_i$ . For the denominator,  $R^+(b_j)$  is the total reproductive output (TRO) of the whole  
 308 population in year  $b_j$ . ERO and TRO are in units of "number of calves" (males and females) here  
 309 (though generally their units are arbitrary but matching). TRO is the total number of adult females  
 310 in the population when  $j$  is born,  $N_{b_j, A}$ , multiplied by the proportion of females with calves (breeding  
 311 state S2),  $\bar{\beta}_2$ :  $R^+(b_j) = \bar{\beta}_2 N_{b_j, A}$ .

312 For the numerator,  $i$ 's ERO has two components: first, she has to survive; second, she has to be  
 313 calving (breeding state 2) in  $b_j$ :

$$R_i(b_j|y_i, a_i) = \Phi(b_j - y_i, a_i) \mathbb{P}[B(a_i + b_j - y_i) = 2], \quad (4)$$

314 where  $\Phi(\Delta t, a)$  gives the probability of survival for  $\Delta t$  years, starting from age  $a$  (product of annual  
 315 juvenile and adult survival probabilities).  $B(a)$  is an individual's breeding state at age  $a$ , which here  
 316 is individual  $i$ 's age at  $b_j$  ( $a_i + b_j - y_i$ ), assuming she survives.

317 Then, using our definition of fecundity at age, Eq. (2), we have

$$\mathbb{P}[K_{ij} = \text{MOP} | a_i, y_i, b_j, L_i = 0, y_i < b_j, \theta] = \frac{\Phi(b_j - y_i, a_i) F(a_i + b_j - y_i)}{N_{b_j, A}}. \quad (5)$$

318 If  $i$  is sampled after the birth of  $j$  ( $b_j < y_i$ ), then  $i$  was either alive at  $j$ 's birth or was not yet  
 319 born, eliminating the need to account for survival or lethality terms. However,  $i$  may not have reached  
 320 reproductive maturity by  $b_j$ . Letting  $F(a \leq 0) = 0$ ,

$$\mathbb{P}[K_{ij} = \text{MOP} | a_i, y_i, b_j, b_j < y_i, \theta] = \frac{F(a_i - (y_i - b_j))}{N_{b_j, A}}. \quad (6)$$

321 **Maternal half-sibling pairs (XmHSPs)** To find probabilities of cross-cohort maternal half-sibling  
 322 pairs (XmHSPs), we check whether individual  $k$  and individual  $l$  have the same mother. We impose  
 323 the following criteria:

324 

- $b_l > b_k$  (avoiding double-counting);

325 

- $b_k \neq b_l$  (because walruses give birth to a single offspring at a time);

326 

- $b_k \geq 2000$  and  $b_l \geq 2000$  (birth years must be greater than or equal to 2000, because population  
 327 dynamics starts at 2000).

328 If we call  $m$  the mother of  $k$ , what is the probability that  $l$ 's mother was  $m$ ? We know that  $m$  was  
 329 alive, mature, and in breeding state S2 at  $k$ 's birth, and that  $m$  survived at least one more year after  
 330  $k$ 's birth, otherwise  $k$  would not have survived (through its dependency on its mother) and would not  
 331 have been sampled. In order for  $m$  to also be  $l$ 's mother, three conditions must be met:

332 1.  $m$  survives until  $b_l + 1$ , because we know  $l$  survived to be sampled at  $1+$  years of age;  
 333 2.  $m$  is in breeding state S2 in  $b_l$ ;  
 334 3. amongst all the females that are alive and in breeding state S2 in year  $b_l$ ,  $m$  is the mother.

335 Let  $\Phi(\Delta t)$  be the adult probability of surviving another  $\Delta t$  years, and recall  $\Psi$  is the breeding cycle  
 336 transition matrix. The three-element probability vector of an animal being in each state (S1, S2, S3) at  
 337 time  $t$  is  $\mathbf{p}^{[t]}$ . Then  $\mathbf{p}^{[t+1]} = \Psi \mathbf{p}^{[t]}$ . Now define  $\mathbf{p}^{[0]} = (0, 1, 0)^\top$  which is the three-element probability  
 338 vector of  $m$ 's breeding state at  $k$ 's birth (certain state 2), let  $B_m(y)$  be  $m$ 's actual breeding state in  
 339 any year  $y$ , and recall  $\bar{\beta}_2$  is the proportion of adult females in breeding state S2. Then

$$\begin{aligned} & \mathbb{P}[K_{kl} = \text{XmHSP} | b_k, b_l, \theta] \\ &= \mathbb{P}[K_{lm} = \text{MOP} | B_m(b_k) = \text{S2}, m \text{ alive at } b_k + 1, b_l, \theta] \\ &= \frac{\Phi(b_l - b_k) [\Psi^{b_l - b_k} \mathbf{p}^{[0]}]_2}{N_{b_l, \text{A}} \bar{\beta}_2}, \end{aligned} \tag{7}$$

340 where  $[\Psi^{b_l - b_k} \mathbf{p}^{[0]}]_2$  is the second element of the vector, i.e., the probability that  $m$  (given she was  
 341 alive) was again in breeding state S2 at  $l$ 's birth.

342 HSPs are one of several “second-order” kin-pairs that are practically indistinguishable genetically  
 343 hence cannot be identified directly and unambiguously. Fortunately, HSPs are demographically by  
 344 far the most common when the birth gap used for comparing samples is short. When the birth gap  
 345 approaches twice the age-of-first-birth, though, grandparent-grandchild pairs (GGPs) become more  
 346 prevalent. To mitigate this issue, we restricted the range of birth gaps considered in the model to  
 347 those where GGPs are rare (or indeed impossible in our simulated data; i.e., below twice the age of  
 348 first birth plus two years).

349 **Self-recaptures (SPs)** Our stage-structured model simplifies population dynamics, but we have  
 350 to make an additional assumption about sampling selectivity to include IMR data. Here, we assume

351 selectivity varies only by stage (adult/juvenile), not by age within stage. We only consider female  
 352 samples for self-recapture, since males are prone to permanent emigration (Beatty et al., 2022), so do  
 353 not yield readily interpretable inferences.

354 To compute stage-structured self-recapture probabilities in a manner analogous to kin capture  
 355 probabilities, we retain only the first and last capture of each individual. This is a reasonable approx-  
 356 imation for walruses because the self-recapture rate is relatively low. We condition on age of the first  
 357 sample ( $a_1$ ) but *not* explicitly on age of the second sample; instead, we condition on the second sam-  
 358 ple's developmental stage at sampling ( $d_2$ ). This is necessary because our model is stage- rather than  
 359 age-structured. If  $d(a)$  is a function that maps age to developmental stage, with  $d(a < 6) =$  "juvenile"  
 360 and  $d(a \geq 6) =$  "adult", then we restrict our comparisons to pairs of samples collected in years  $y_1$  and  
 361  $y_2$  where:

$$d(a_1 + (y_2 - y_1)) = d_2. \quad (8)$$

362 If, based on age of the first sample ( $a_1$ ) and time elapsed between sampling events ( $y_2 - y_1$ ) the first  
 363 sample would have reached the developmental stage of the second sample ( $d_2$ ; i.e., the two could be  
 364 the same animal), then we assume it is equally likely to be *any* of the females in that developmental  
 365 stage in that year. Therefore, the probability that the first sample is the same individual as the second  
 366 sample is the reciprocal of the developmental stage abundance. Additionally, we account for survival  
 367 over the intervening years. The self-recapture kinship probability between samples 1 and 2 (where  
 368  $y_1 < y_2$ ) is:

$$\mathbb{P}[K_{12} = \text{SP} | a_1, y_1, d_2, y_2, L_1 = 0, \boldsymbol{\theta}] = \frac{\mathbb{I}[d(a_1 + (y_2 - y_1)) = d_2] \Phi(y_2 - y_1, a_1)}{N_{y_2, d_2}}. \quad (9)$$

369 The survival term  $\Phi(y_2 - y_1, a_1)$  represents the probability of survival for  $\Delta t$  years as defined in section  
 370 2.1.3. We also condition on the first sample being non-lethal (since the individual was subsequently  
 371 recaptured). To obtain  $N_{y_2, d_2}$ , we need either adult or juvenile abundance. Adult abundance is  
 372 included in the population dynamics model, however, additional steps are required to deduce juvenile  
 373 abundance. Assuming stable age composition, we show in Appendix S1: Section S3 that for walruses:

$$N_{y, J} = N_{y, A} \frac{\lambda - \phi_A}{\lambda - \phi_J} \left( \left( \frac{\lambda}{\phi_J} \right)^5 - 1 \right), \quad (10)$$

374 where  $\lambda = e^r$  is the relative annual population growth rate.

375 **2.1.4 Pseudo-likelihood**

376 Given a real dataset, we would maximize the pseudo-log-likelihood that combines kinship probabilities  
377 and actual outcomes of all pairwise comparisons to estimate demographic parameters. To define the  
378 pseudo-log-likelihood, in brief, let  $w_{ijk}$  be “the data”, i.e. the kinship outcome, for samples  $i$  and  $j$   
379 and target kinship  $k$ :  $w_{ijk} = 1$  if the actual kinship  $K_{ij} = k$ , or  $w_{ijk} = 0$  if  $K_{ij} \neq k$ . As shown in  
380 Bravington et al. (2016), for “sparse sampling” CKMR where the population is large and the sampling  
381 fraction is correspondingly small, the comparisons are approximately statistically independent. Define  
382  $p_{ijk}(\boldsymbol{\theta}) = \mathbb{P}[K_{ij} = k | z_i, z_j, \boldsymbol{\theta}]$  to be the kinship probability for samples  $i$  and  $j$ , parameter values  $\boldsymbol{\theta}$  and  
383 covariates  $z_i$  and  $z_j$  (computed from, e.g., Eq. (5)). In each case, the probability that  $w_{ijk} = 1$  is on  
384 the order of the reciprocal of adult abundance, which is very small, and therefore the pseudo-likelihood  
385  $L$  is well approximated by a Poisson distribution with mean  $p_{ijk}(\boldsymbol{\theta})$ :

$$w_{ijk} \sim \text{Poisson}(p_{ijk}(\boldsymbol{\theta}))$$

$$L(\boldsymbol{\theta}; w) = C \prod_{i < j; k \in \mathcal{K}} e^{-p_{ijk}(\boldsymbol{\theta})} p_{ijk}(\boldsymbol{\theta})^{w_{ijk}}, \quad (11)$$

386 where  $C$  is a constant and  $\mathcal{K}$  are the kinship relationships being considered. Let  $w = \{w_{ijk}; \forall i, j, k\}$ ,  
387 the possible combinations of samples and kin relationships; although in practice, some “impossible”  
388 comparisons are excluded (e.g., second-order kin born a long time apart). Then, the pseudo-log-  
389 likelihood is:

$$\log_e L(\boldsymbol{\theta}; w) = \Lambda(\boldsymbol{\theta}; w) = C + \sum_{i < j; k \in \mathcal{K}} \{-p_{ijk}(\boldsymbol{\theta}) + w_{ijk} \log_e p_{ijk}(\boldsymbol{\theta})\}. \quad (12)$$

390 **2.1.5 Design calculations**

391 For design purposes, we use an analytical method to predict precision of the estimates expected under  
392 different sampling scenarios. The parameter uncertainty likely to result from proposed CKMR sam-  
393 pling designs can often be evaluated by calculation alone (Bravington et al., 2016, section 5). These  
394 calculations are adaptations of standard methods used to find the statistical information (i.e., deriva-  
395 tives) from the pseudo-log-likelihood, combined with enumerating the pairwise comparisons that would  
396 be available per covariate combination (which are limited here to: age or stage, sample year, and sex).

397 The statistical basis is given in Bravington et al. (2016), section 4. Following standard statistical  
398 practice, we approximate the parameter variance using the inverse of the (pseudo) Fisher Information

399  $H(\boldsymbol{\theta}_0) = -\mathbb{E}_W [d^2 \Lambda(\boldsymbol{\theta}_0; W) / d\boldsymbol{\theta}^2]$  (the negative expected Hessian over datasets evaluated at true parameter values  $\boldsymbol{\theta}_0$ , which are taken from the simulation). As  $\Lambda(W)$  is a sum of individual comparison 400 terms, we can also write  $H(\boldsymbol{\theta}_0) = \sum_{i < j; k \in \mathcal{K}} h_{ijk}(\boldsymbol{\theta}_0)$ , where  $h_{ijk}(\boldsymbol{\theta}_0)$  is the expected Fisher information 401 matrix from a single comparison of type  $(i, j, k)$ . Further, Appendix S1: Section S4 shows that 402 for Poisson random variables such as  $w_{ijk}$ , we have 403

$$h_{ijk}(\boldsymbol{\theta}_0) = 4\Delta_{ijk}(\boldsymbol{\theta}_0)\Delta_{ijk}(\boldsymbol{\theta}_0)^\top \quad \text{where } \Delta_{ijk}(\boldsymbol{\theta}) = \frac{d\sqrt{p_{ijk}(\boldsymbol{\theta})}}{d\boldsymbol{\theta}}. \quad (13)$$

404 The vector  $\Delta_{ijk}(\boldsymbol{\theta})$  can therefore be obtained for all  $(i, j, k)$  by numerical differentiation of the probabilities 405 calculated by the ICKMR model.

406 We now group across pairs with identical covariate values. Let  $m(\mathbf{z})$  denote the number of samples 407 with covariate combination  $\mathbf{z}$ ; the number of comparisons between two samples is  $m(\mathbf{z}_1)m(\mathbf{z}_2)$  (ignoring 408 double-counting for the moment). The grouped version of the pseudo-Fisher information can 409 be written as

$$H(\mathbf{m}_{\mathcal{Z}}; \boldsymbol{\theta}_0) = \sum_{\mathbf{z}_1, \mathbf{z}_2 \in \mathcal{Z}; k \in \mathcal{K}} \left( \mathbb{I}(\mathbf{z}_1 < \mathbf{z}_2) + \frac{1}{2}\mathbb{I}(\mathbf{z}_1 = \mathbf{z}_2) \right) m(\mathbf{z}_1)m(\mathbf{z}_2) h_{\mathbf{z}_1 \mathbf{z}_2 k}(\boldsymbol{\theta}_0), \quad (14)$$

410 where the parentheses containing indicators handle double counting in the  $m(\mathbf{z}_1)m(\mathbf{z}_2)$  product and 411  $h_{\mathbf{z}_1 \mathbf{z}_2 k}(\boldsymbol{\theta}_0)$  gives the Fisher information matrix for two samples with covariates  $\mathbf{z}_1$  and  $\mathbf{z}_2$  and kinship 412  $k$ .  $\mathcal{Z}$  gives the collection of covariate combinations (analogous to  $\mathcal{K}$  for the kinships) and  $\mathbf{m}_{\mathcal{Z}}$  gives the 413 sample sizes for those combinations (i.e.,  $\mathbf{m}_{\mathcal{Z}}$  is a vector as long as there are covariate combinations 414 in  $\mathcal{Z}$  and each element is the number of samples for that covariate combination).

415 We then invert matrix  $H(\mathbf{m}_{\mathcal{Z}}; \boldsymbol{\theta}_0)$  to approximate the expected variance  $V(\mathbf{m}_{\mathcal{Z}}; \boldsymbol{\theta}_0)$  of a parameter 416 estimate. Uncertainty from any function of the parameters,  $g(\boldsymbol{\theta})$ , can then be approximated by the 417 delta method:

$$\mathbb{V}[g(\boldsymbol{\theta}); \mathbf{m}_{\mathcal{Z}}, \boldsymbol{\theta}_0] \approx \left[ \frac{dg(\boldsymbol{\theta})}{d\boldsymbol{\theta}} \Big|_{\boldsymbol{\theta}_0} \right] V(\mathbf{m}_{\mathcal{Z}}, \boldsymbol{\theta}_0) \left[ \frac{dg(\boldsymbol{\theta})}{d\boldsymbol{\theta}} \Big|_{\boldsymbol{\theta}_0} \right]^\top. \quad (15)$$

418  $\boldsymbol{\theta}_0$  values for annual sample sizes and number of years of sampling come directly from our designs; 419 however, the age-sex composition of the samples comes from our simulations.

420 The realized adult sample size (about 1,100 per year for 2013-2017 and 2023, or 6,600 total to 421 date) is large enough relative to adult female abundance ( $\sim 70,000$ ; effectively more because of turnover

422 during the years modelled) that  $\sim 5\text{--}10\%$  of samples are self/kin-recaptures. This means that a con-  
423 siderable proportion of pairwise comparisons have predictable outcomes based on the results of other  
424 comparisons, breaking independence. The “sparse sampling” assumption of Bravington et al. (2016)  
425 is therefore not strictly justified, so the variance might be slightly over- or under-estimated relative  
426 to our calculations. The direction is not entirely obvious, because finite population corrections will  
427 also affect the true variance, but we chose to eliminate redundant comparisons to err on the side of  
428 over-estimating true variance. Specifically:

429 1. If an animal  $i$  was recaptured in multiple years, we only used  $i$ ’s last recapture in MOP and  
430 XmHSP comparisons;

431 2. If a sample  $j$  was identified as the offspring in a MOP, we did not use it in XmHSP comparisons  
432 (because the outcome of an XmHSP comparison between  $j$  and any other sample  $k$  could be  
433 deduced from  $j$  and  $k$ ’s MOP results;  $k$  and  $j$  are XmHSP if  $k$  was another offspring of  $j$ ’s  
434 mother).

435 Eliminating these comparisons means that we must adjust the effective sample sizes  $\mathbf{m}_{\mathcal{Z}}$  accordingly.  
436 We used simulation results on the frequency of self-recaptures and MOPs to determine how many  
437 samples would need to be eliminated and found that the effect is small for the scenarios we considered.

## 438 2.2 Simulation for model checking and design scenarios

### 439 2.2.1 Simulations

440 To test our ICKMR model, we developed an individual-based simulation with walrus life history,  
441 modified from the R (R Core Team, 2025) package fishSim (Baylis, 2019). The simulation is stochastic  
442 and operates on an annual basis. Individuals are tracked using unique identifiers allowing identification  
443 of kinship pairs in simulated samples. We ran the simulation from 1950 to 2030, using an initial  
444 population of 250,000 animals. These individuals are considered “founders” and do not have mothers  
445 or fathers. The age and sex structure of the initial population is determined by survival and fecundity  
446 rates used in the simulation (Table 1), which were based on estimated 2015 rates (Taylor et al., 2018).  
447 Parameters in Table 1 were adjusted to maintain the desired population growth rate ( $e^r$ ). Individuals  
448 of breeding age mate randomly and males can potentially father more than one calf per year. Female  
449 reproduction is as described in Section 2.1.2. Females that are in state 2 of the breeding cycle give  
450 birth to a single offspring with 1:1 sex ratio (Fay, 1982). There is no systematic age effect on female

451 reproductive dynamics, except that they are guaranteed not pregnant at 4 years of age when they  
452 enter the breeding cycle (Section 2.1.2), which slightly lowers effective fecundity for the first few  
453 years of adulthood until the Markov chain reaches equilibrium. We did not include senescence in our  
454 ICKMR model, but we did include it in our simulations so we could investigate effects of violating the  
455 assumption of “no senescence” in the ICKMR model.

456 In sampling years, captures are simulated according to either historical or planned future sample  
457 sizes (Table 2). Females are available to be sampled at any age 1+, while males are available for  
458 sampling from ages 1-5 only, because adult males do not tend to travel to the Chukchi Sea in the  
459 summer. After sampling, some individuals die (according to age and/or sex specific mortality rates,  
460 Table 1). If a female with a YOTY dies, her calf also dies. Individuals automatically die if they reach  
461 the maximum age. Living individuals then have their age incremented.

462 The breeding probability/birth rate is confounded with the YOTY survival rate. Because only  
463 samples from age 1 onwards are considered, only the product (nominal breeding probability rate  $\times$   
464 nominal YOTY survival) affects the simulated samples, not the two constituent parameters. The  
465 simulation then proceeds to the following year.

#### 466 2.2.2 Model checking

467 To evaluate agreement between the simulation and ICKMR model, we simulated 50 replicate datasets  
468 with demographic parameters under a null scenario (D0, Table 1), and we simulated historical and  
469 future sampling according to realized or target sample sizes by age class, with effort per year constant  
470 at the 2023 level (S0, Table 2). The population dynamics model in the simulations is close (but not  
471 identical) to the ICKMR model because the simulation includes a definite maximum age, whereas the  
472 ICKMR model does not. We checked each of the simulated datasets against the ICKMR model for:  
473 observed (i.e., simulated) and expected numbers of kin pairs in different categories (MOPs, XmHSPs,  
474 and SPs); observed versus expected year gaps between half-sibling pairs, unbiasedness of the log-  
475 likelihood derivatives at the true parameter values, and parameter bias. These comparisons enabled  
476 us to evaluate whether the simulation and ICKMR models were consistent and whether simplifications  
477 made in the ICKMR model were acceptable. Refer to Appendix S1: Section S5 for details.

478 **2.2.3 Scenarios**

479 We evaluated the performance of ICKMR under different demographic and sampling scenarios. The  
480 demographic scenarios were a stationary population (D1), a slightly decreasing population (D2) and  
481 a slightly increasing population (D3) (Table 1). These values were chosen because they represent the  
482 credibility limits and point estimate for the 2015 walrus population growth rate based on an integrated  
483 population model (Taylor et al., 2018). We simulated historical sampling (2013-2017, when the first  
484 generation of research expeditions took place) according to realized sample sizes by age and sex (Beatty  
485 et al., 2022). We simulated possible reductions in future sampling effort, either by reducing the number  
486 of sampling years or by reducing the amount of sampling effort within years (S1-S8; Table 2). For  
487 simulated captures between 2023 and 2028, we estimated an expected overall sample size of 1600  
488 per year with 100% effort (i.e., a four-week research expedition). We estimated that 75% effort (a  
489 three-week research expedition) would result in an expected sample size of 1200. Planned sampling  
490 went ahead in 2023 but not in 2024, so we modified simulated sampling scenarios 1-8 to represent the  
491 “reality” of 100% survey effort in 2023 and 0% survey effort in 2024.

492 The FWS Walrus Harvest Monitoring Program (WHMP) monitors the walrus harvest each year  
493 in two coastal communities in Alaska, which comprises 84% of total Alaska Native subsistence harvest  
494 (MacCracken et al., 2017). WHMP collects demographic data and biological samples from harvested  
495 animals. To assess the relative value of samples from harvested animals (versus biopsy samples from  
496 live individuals), we simulated each scenario without (L1) and with (L2) the substitution of 500 live  
497 biopsy samples with 500 lethal samples in sampling years 2023-2028.

498 With three demographic scenarios, eight sampling scenarios, and two lethality scenarios, this re-  
499 sulted in a total of 48 simulated datasets from which to evaluate survey design. Given the relatively  
500 large population size and large number of samples, we did not expect key properties of simulated  
501 datasets to differ substantially due to random variation. This was confirmed by model checking (refer  
502 to Appendix S1: Section S5). Therefore, we evaluated a single realization of each simulated  
503 scenario.

504 Beatty et al. (2022) achieved a CV of 0.19 on adult female abundance in a five-year study. With  
505 this result in mind, we compared the estimated CVs for adult female abundance derived from IMR  
506 and ICKMR models to precision benchmarks of CV = 0.20, CV = 0.10 (representing a 50% reduction  
507 in CV), and CV = 0.05 (representing a 75% reduction in CV). Thus, we evaluated performance of our  
508 IMR and ICKMR models relative to performance of a multievent model with sampling effort over five

509 years (2013-2017).

## 510 3 Results

### 511 3.1 Adult female abundance

512 Across all sampling scenarios, ICKMR gave substantially more precise abundance estimates than IMR  
513 alone (Fig. 2). This was also true across demographic scenarios (refer to Appendix S1: Figure S4 and  
514 Appendix S1: Table S4). The mean absolute decrease in CV on adult female abundance in paired  
515 scenarios with IMR and ICKMR was 7% for a stationary population, 4% for a decreasing population,  
516 and 8% for an increasing population. These represent relative decreases in CV of 47%, 45%, and 47%  
517 respectively. Refer to Appendix S1: Table S4 for expected CVs of adult female abundance across all  
518 demographic and sampling scenarios with and without the substitution of lethal samples and use of  
519 CKMR.

520 The demographic scenarios (refer to Table 1) affected expected precision. With a declining popu-  
521 lation and smaller resulting population size during target inference years, there is less competition to  
522 be the kin of any given sample, therefore the number of kin pairs is higher, reducing the expected CV  
523 for a given sample size. The opposite happens with an increasing population.

524 The simulated sampling scenarios resulted in between 1.75 and 5 years of total survey effort between  
525 2023 and 2028 (where total survey effort is a combination of years of effort and effort per year, which  
526 may be fractional, and where 5 years of total survey effort between 2023 and 2027 was the original  
527 plan for IMR; Fig. 3). In general, expected CVs on adult female abundance decreased with increasing  
528 number of total sampling years (Fig. 3). For a simulated stationary population and with a target  
529 CV of 0.2 (similar to CV = 0.19 from the IMR analysis in Beatty et al., 2022) on estimates of adult  
530 female abundance in 2025, sufficient precision was achieved in all sampling scenarios with ICKMR  
531 with or without the substitution of lethal samples (Fig. 2 and Fig. 3). For IMR with or without the  
532 substitution of lethal samples at least 3 years of total survey effort would be required to achieve a CV  
533 of 0.2. With a target CV of 0.1, ICKMR could achieve sufficient precision with 4 years of total survey  
534 effort, while IMR alone would not achieve this precision even with 5 years of total survey effort.

535 The simulated substitution of 500 lethal samples per sampling year slightly changed expected  
536 precision in abundance estimates (the mean change in CV with versus without lethal samples was  
537 <1% across all demographic and sampling scenarios, with a maximum increase of 3%). For ICKMR,

538 expected CVs on adult female abundance were consistently higher when lethal samples were used, but  
539 the magnitude of the difference was small (mean increase of 0.14%). This suggests that lethal samples  
540 are almost equally valuable for walrus ICKMR, and the substitution of lethal samples for live biopsy  
541 samples could reduce required expedition length (500 samples = approx. 1/3 of samples expected  
542 during a 4-week expedition).

### 543 3.2 Demographic parameters

544 The simulated values of adult female survival and post-senescent adult female survival (Table 1)  
545 resulted in effective survival from age 6-37 of 0.96, 0.95, and 0.96 for stationary, decreasing, and  
546 increasing populations, respectively. Depending on demographic scenario, sampling scenario, and  
547 substitution of lethal samples, the expected SEs on adult female survival ranged from 0 to 0.03. When  
548 estimated with ICKMR, the expected SEs on adult female survival were always lower than when IMR  
549 alone was applied (mean decrease in SE = 0.01). The simulated values of juvenile female survival from  
550 age 1-5 were 0.9, 0.85, and 0.925 (Table 1). Across demographic scenarios, sampling scenarios, and  
551 the substitution of lethal samples, the expected SEs on juvenile female survival ranged from 0.02 to  
552 0.06. The mean expected decrease in SE on juvenile female survival with ICKMR was 0.01. Across  
553 all demographic and sampling scenarios, the simulated proportion of adult females in breeding state  
554 2 (calving) was 0.26. The mean expected SEs on the proportion of adult females in breeding state 2  
555 across demographic, sampling and lethality scenarios was 0.11 (range 0.01-0.31). The expected SEs  
556 on the proportion of adult females in breeding state 2 were notably lower when ICKMR was used  
557 compared with IMR (mean decrease in SE = 0.19). Refer to Appendix S1: Table S3 for expected  
558 SEs of life history parameters across all demographic and sampling scenarios with and without the  
559 substitution of lethal samples and use of ICKMR.

## 560 4 Discussion

561 We developed an ICKMR study design, with walrus as a case study, as an example for other researchers  
562 embarking on this evolving type of study. We investigated whether using ICKMR could increase  
563 expected precision in estimates of adult female walrus population size. To do this, we developed an  
564 ICKMR model with individual recaptures as a kin type (self pairs, SP) in addition to mother-offspring  
565 and cross-cohort maternal half-sibling pairs (MOPs and XmHSPs). We made simplifying assumptions

566 for tractability. For example, we decided to exclude paternal kinships and not to model males at all  
567 because there would be minimal information in the data and extra complications in the modelling;  
568 we opted for a stage-structured (rather than age-structured) model, assuming unselective sampling by  
569 age within stage (which may not be particularly accurate for juveniles). In the future, a fully age-  
570 structured version of the model would simplify the kinship probabilities for the self-recapture data. We  
571 further assumed quasi-equilibrium population dynamics across the period 2000–2028, with a constant  
572 rate of population change and stable age composition. This is a simplification during at least part of  
573 the time frame (Taylor et al., 2018). Nevertheless, given that our general purpose was to investigate  
574 sample size requirements, we believe our simplifications were reasonable.

575 The walrus project was initially planned as an IMR project with five years of total survey effort  
576 between 2013 and 2017 and another five years planned between 2023 and 2027. Because the 2023  
577 survey went ahead, we considered that year as fixed in our design scenarios. For all demographic  
578 scenarios, we found that expected relative CVs on adult female abundance were substantially (>30%)  
579 and consistently lower when using ICKMR than when using IMR. Our results indicated that by adding  
580 CKMR, a CV of 0.2 on estimates of adult female population size in 2025 could be achieved with 1.75  
581 years of survey effort between 2023 and 2028, whereas IMR alone would require at least 3 years of  
582 total survey effort within this period (with planned sample sizes per year of 1600; Fig. 3). Because  
583 this expected CV applies to adult females only, decision makers may wish to set a lower target CV; for  
584 example, with a target CV of 0.1, 4 years of total survey effort would be required with ICKMR but  
585 would not be achievable within 5 years with IMR alone. Estimates of adult female and juvenile female  
586 survival, and of the proportion of adult females in breeding state 2 (calving), were also improved with  
587 the addition of CKMR.

588 Lethal samples can be incorporated into both IMR and CKMR analyses. In this study, we con-  
589 sidered lethal samples as a potential replacement for some live samples, and assumed that lethal and  
590 non-lethal samples were similar in terms of ERRO. Partial substitution of lethal samples for non-lethal  
591 (biopsy) samples resulted in similar precision on abundance estimates. In previous years, 50 samples  
592 per year were collected from harvested animals by the FWS WHMP. However, the total harvest in  
593 Alaska and Russia is estimated to number ~4,210 walruses per year (mean for 2016-2020; US Fish and  
594 Wildlife Service, 2023). Approximately 400 harvested samples would be needed to reduce each cruise  
595 by one week or 1600 samples would be needed to remove the need for an entire cruise. We did not  
596 investigate the impact of using exclusively harvested samples in place of one or more survey years, nor

597 did we investigate the potential consequences of hunter preferences (e.g., if hunters preferentially target  
598 large adult females, and those females tend to be more fecund, the ERRO of lethal and non-lethal  
599 samples may not be the same). In the longer term, using exclusively lethal samples could lead to lower  
600 precision in estimates of abundance, because lethal samples cannot go on to be self-recaptures or fu-  
601 ture parents. Using samples from harvested walruses in combination with non-lethal samples collected  
602 from wild animals during research cruises can increase cost efficiency by reducing the need for extended  
603 at-sea operations, thereby lowering logistical expenses associated with vessel charters and personnel  
604 time. Additionally, partial reliance on harvested samples mitigates disturbance to live walruses by  
605 decreasing the need for direct interactions with animals in the wild. This approach also strengthens  
606 collaboration with Alaska Native hunters and co-management partners, fostering cooperative research  
607 efforts that align with subsistence practices and local ecological knowledge. For example, further work  
608 could be done in collaboration with the WHMP to better understand hunter preferences and to in-  
609 corporate these into the CKMR model. Such partnerships are essential for long-term monitoring and  
610 effective management of the species. Furthermore, the ongoing contribution of the WHMP to walrus  
611 abundance estimation provides a strong justification for maintaining the program, ensuring that robust  
612 population assessments continue to inform conservation and management decisions.

613 The results presented here all assume that age is accurately measured for each sample, using a  
614 DNA methylation-based “epigenetic clock”. Although epigenetic age has been shown to work fairly  
615 well in a variety of species, including walruses as in Robeck et al. (2023a), and further calibration  
616 studies are ongoing to improve cost and precision, epigenetic age is not perfectly precise. Failure to  
617 allow for any ageing error in CKMR will certainly lead to bias; for example, the birth-gap between  
618 XHSPs will be systematically overestimated, so that mortality rates will be underestimated. However,  
619 as long as the error variance of estimated age is known, it is possible to allow for ageing error within  
620 the CKMR probability formulas, using weighted sums over kinship probabilities at different true ages.  
621 This should eliminate bias (Petersma et al., 2024), and Thomson et al. (2020) followed this approach  
622 for school shark (*Galeorhinus galeus*) using vertebral ages rather than epigenetic ages. In the case  
623 of ICKMR, the information from recaptured individuals will also be useful in resolving ages, because  
624 the interval between sampling will be known. Nevertheless, in severe cases, uncertainty about age  
625 can drastically limit the ability to gain information from CKMR, even when the number of kin-pairs  
626 found is high and the model is adjusted properly, as noted from practical experience by Trenkel et al.  
627 (2022). We expect to include ageing error in our ICKMR model when data are available and expect

628 that doing so will reduce precision compared to having hypothetical perfect age information. The loss  
629 of precision can be investigated through our design framework, but we opted not to include it in our  
630 design calculations (i.e., we assumed that there is no error), because we do not yet know how large  
631 the errors will be. Design calculations can be easily re-run when better estimates of ageing error are  
632 available. For that purpose, a fully-age-structured, rather than stage-structured model, would avoid  
633 the need to map uncertainty in age estimates to uncertain developmental stages.

634 The basic assumptions of CKMR are that each animal had one mother and one father, and that  
635 the types of close-kin used in the model (generally first- and/or second-order) can be reliably identified  
636 genetically. While most vertebrates meet these requirements, the practical considerations of sampling  
637 mean that it would not be sensible to apply CKMR to some species and populations. Design exercises  
638 like the one presented here can help quantify cost and effort needed to achieve sufficient precision in  
639 quantities of interest using CKMR.

640 Because CKMR is a flexible modeling framework, and because sampling can be done in so many  
641 different ways, it is almost impossible to make absolute pronouncements about a species' suitability  
642 for CKMR, except in relation to some particular sampling scheme. For example, lethal sampling of  
643 persistent family groups, as in wolves (Canidae) or killer whales (*Orcinus orca*), would be unlikely  
644 to yield useful results. CKMR tends to work best for relatively large, well-mixed populations, where  
645 sampling is sparse and approximate independence of comparisons is reasonable (refer to Bravington  
646 et al., 2016 for additional details). For any pairwise comparison used in the model, there should be  
647 no unmodeled correlation between sampling probability and reproduction, or between the event of  
648 an individual's being sampled and its expected number of sampled close-kin. Sometimes this can be  
649 achieved by excluding certain pairwise comparisons from the model (e.g., between animals sampled  
650 close together in space and time, as for school shark in Thomson et al., 2020); sometimes by building  
651 a more elaborate model that conditions on covariates like place and time of sampling, thus avoiding  
652 the "unmodeled" issue. Here, for walruses, we assumed that if a mother is sampled, any accompanying  
653 offspring are likely nearby and therefore have increased sampling probability, which would violate the  
654 condition above. Therefore, we did not compare possible offspring and mothers sampled in the same  
655 year unless the potential offspring was definitely not accompanying its mother; i.e., the offspring was  
656 sampled as an adult. These examples underscore the need to work closely with biologists to incorporate  
657 accurate information about the life-history of the species of interest in CKMR model development.

658 Results described in this paper fully leverage CKMR to further advance population ecology. We

659 demonstrate how CKMR can be combined with IMR into a unified model and substantially increase  
660 precision in estimates of population size and demographic parameters compared to IMR alone. We  
661 provide an example of ICKMR study design, including model development, model checking, and design  
662 calculations, and show how simulated data can be used to evaluate different proposed survey designs.  
663 While we used walrus as a motivating example, we expect that ICKMR can be used for estimating  
664 population parameters of interest across a range of taxa.

665 **Acknowledgments**

666 Funding was provided by the USGS Science Support Partnership program. The findings and conclu-  
667 sions in this article are those of the authors and do not necessarily represent the views of the U.S.  
668 Fish and Wildlife Service. Any use of trade, product or firm names is for descriptive purposes only  
669 and does not imply endorsement by the United States Government. We thank Paul Conn and two  
670 anonymous reviewers for helpful feedback on earlier versions of this manuscript.

671 **Author contributions**

672 Conceptualization: EKJ, MVB, RLT, IST, DLM, WSB. Data curation: EKJ. Formal analysis: EKJ,  
673 MVB. Funding acquisition: RLT, IST, WSB. Investigation: EKJ, MVB. Methodology: EKJ, MVB.  
674 Project administration: EKJ, DLM, WSB. Software: EKJ, MVB, DLM. Supervision: EKJ, DLM,  
675 WSB. Validation: EKJ, MVB, RLT. Visualization: EKJ, MVB. Writing – original draft: EKJ, MVB,  
676 RLT. Writing – review & editing: EKJ, MVB, RLT, IST, DLM, WSB.

677 **Conflict of interest statement**

678 The authors declare no conflicts of interest.

679 **References**

680 Baylis, S. M. (2019). *fishSim: R Tool for Simulation of Fish Population Dynamics*. <https://github.com/SMBaylis/fishSim>. Accessed 2025-12-11.

681

682 Beatty, W. S. et al. (2020). “Panmixia in a sea ice-associated marine mammal: evaluating genetic  
683 structure of the Pacific walrus (*Odobenus rosmarus divergens*) at multiple spatial scales”. In: *Journal  
684 of Mammalogy* 101.3, pp. 755–765.

685 Beatty, W. S. et al. (2022). “Estimating Pacific walrus abundance and survival with multievent mark-  
686 recapture models”. In: *Marine Ecology Progress Series* 697, pp. 167–182.

687 Bravington, M. V., H. J. Skaug, and E. C. Anderson (2016). “Close-Kin Mark-Recapture”. In: *Statistical  
688 Science* 31.2, pp. 259–274.

689 Bravington, M. V., S. Jarman, and H. Skaug (2014). *Antarctic Blue Whale surveys: augmenting via  
690 genetics for close-kin and ordinal age*. Scientific Committee paper SC/65b/SH17. International  
691 Whaling Commission.

692 Caswell, H. (2001). *Matrix Population Models: Construction, Analysis, and Interpretation*. en. 2nd  
693 Edition. Sunderland, Massachusetts, USA: Sinauer Associates, Inc.

694 Conn, P. B. et al. (2020). “Robustness of close-kin mark–recapture estimators to dispersal limitation  
695 and spatially varying sampling probabilities”. In: *Ecology and Evolution* 10.12, pp. 5558–5569.

696 Davies, C. et al. (2020). *Next-generation Close-kin Mark Recapture: Using SNPs to identify half-sibling  
697 pairs in Southern Bluefin Tuna and estimate abundance, mortality and selectivity*. FRDC report  
698 2016-044. CSIRO.

699 Fay, F. H. (1982). “Ecology and biology of the Pacific walrus, *Odobenus rosmarus divergens* Illiger”.  
700 In.

701 — (1985). “*Odobenus rosmarus*”. In: *Mammalian Species* 238, pp. 1–7.

702 Fay, F. H., B. P. Kelly, and J. L. Sease (1989). “Managing the Exploitation of Pacific Walruses: A  
703 Tragedy of Delayed Response and Poor Communication”. In: *Marine Mammal Science* 5.1, pp. 1–  
704 16.

705 Fay, F. H. et al. (1997). *Status of the Pacific Walrus Population, 1950–1989*. Tech. rep. 4. U.S. De-  
706 partment of the Interior, U.S. Fish and Wildlife Service, Marine Mammals Management, pp. 537–  
707 565.

708 Gilbert, J. R. (1999). “Review of previous Pacific walrus surveys to develop improved survey designs”.  
709 In: *Marine Mammal Survey and Assessment Methods*. CRC Press.

710 Hillary, R. et al. (2018). "Genetic relatedness reveals total population size of white sharks in eastern  
711 Australia and New Zealand". In: *Nature Scientific Reports* 8 (1), p. 2661.

712 Jay, C. V., A. S. Fischbach, and A. A. Kochnev (2012). "Walrus areas of use in the Chukchi Sea during  
713 sparse sea ice cover". In: *Marine Ecology Progress Series* 468, pp. 1–13.

714 Johnson, D. L. et al. (2024a). "Assessing the Population Consequences of Disturbance and Climate  
715 Change for the Pacific Walrus". In: *Marine Ecology Progress Series* 740, pp. 192–211.

716 Johnson, D. L. et al. (2024b). "Assessing the sustainability of Pacific walrus harvest in a changing  
717 environment". In: *The Journal of Wildlife Management*, e22686.

718 Katsumata, E. et al. (2020). "Growth and reproduction of captive Pacific Walrus (*Odobenus rosmarus*  
719 *divergens*)". In: *Veterinary Integrative Sciences* 18.2, pp. 85–102.

720 Keyfitz, N. and H. Caswell (2005). *Applied mathematical demography*. Springer.

721 Kryukova, N. (2014). "The method of age determination of the Pacific walrus (*Odobenus rosmarus*  
722 *divergens*) using the layered structure of functional teeth". In: *Biology Bulletin* 41, pp. 681–689.

723 Lloyd-Jones, L. R. et al. (2023). "Close-kin mark-recapture informs critically endangered terrestrial  
724 mammal status". In: *Scientific Reports* 13.1, p. 12512.

725 MacCracken, J. G. et al. (2017). *Final Species Status Assessment for the Pacific Walrus*. Tech. rep.  
726 U.S. Department of the Interior, U.S. Fish and Wildlife Service, Marine Mammals Management.

727 Merriell, B. D., M. Manseau, and P. J. Wilson (2024). "Assessing the suitability of a one-time sampling  
728 event for close-kin mark-recapture: A caribou case study". In: *Ecology and Evolution* 14.9, e70230.

729 Palsbøll, P. J. et al. (1997). "Genetic tagging of humpback whales". In: *Nature* 388.6644, pp. 767–769.

730 Petersma, F. T. et al. (2024). "Age is not just a number: How incorrect ageing impacts close-kin  
731 mark-recapture estimates of population size". In: *Ecology and Evolution* 14.6, e11352.

732 Polanowski, A. M. et al. (2014). "Epigenetic estimation of age in humpback whales". In: *Molecular  
733 Ecology Resources* 14.5, pp. 976–987.

734 R Core Team (2025). *R: A Language and Environment for Statistical Computing*. Version 4.5.2. Vienna,  
735 Austria: R Foundation for Statistical Computing.

736 Robeck, T. R. et al. (2022). "Growth, maturity, reproduction, and life expectancy in ex-situ pacific  
737 walruses (*Odobenus rosmarus divergens*)". In: *BMC Zoology* 7.1, p. 57.

738 Robeck, T. R. et al. (2023a). "Multi-tissue DNA methylation aging clocks for sea lions, walruses and  
739 seals". In: *Communications Biology* 6.359.

740 Robeck, T. R. et al. (2023b). "Multi-tissue DNA methylation aging clocks for sea lions, walruses and  
741 seals". In: *Communications Biology* 6.1, p. 359.

742 Sévèque, A. et al. (2024). "Sources of bias in applying close-kin mark–recapture to terrestrial game  
743 species with different life histories". In: *Ecology* 105.3, e4244.

744 Silber, G. K. and J. D. Adams (2019). "Vessel Operations in the Arctic, 2015–2017". In: *Frontiers in  
745 Marine Science* 6.

746 Skaug, H. J. (2001). "Allele-Sharing Methods for Estimation of Population Size". In: *Biometrics* 57.3,  
747 pp. 750–756.

748 Speckman, S. G. et al. (2011). "Results and evaluation of a survey to estimate Pacific walrus population  
749 size, 2006". In: *Marine Mammal Science* 27.3, pp. 514–553.

750 Swenson, J. D. et al. (2024). "Accounting for unobserved population dynamics and aging error in  
751 close-kin mark-recapture assessments". In: *Ecology and Evolution* 14.2, e10854.

752 Taras, B. D. et al. (2024). "Estimating Demographic Parameters for Bearded Seals, *Erignathus bar-  
753 batus*, in Alaska Using Close-Kin Mark-Recapture Methods". In: *Evolutionary Applications* 17.11,  
754 e70035.

755 Taylor, R. L. and M. S. Udevitz (2015). "Demography of the Pacific walrus (*Odobenus rosmarus  
756 divergens*): 1974–2006". In: *Marine Mammal Science* 31.1, pp. 231–254.

757 Taylor, R. L. et al. (2018). "Demography of the Pacific walrus ( *Odobenus rosmarus divergens* )  
758 in a changing Arctic". In: *Marine Mammal Science* 34.1, pp. 54–86.

759 Thomson, R. et al. (2020). *Close kin mark recapture for School Shark in the SESSF*. FRDC Report  
760 2007/034. CSIRO, Australia.

761 Trenkel, V. M. et al. (2022). "Close-kin mark-recapture abundance estimation: practical insights and  
762 lessons learned". In: *ICES Journal of Marine Science*.

763 Udevitz, M. S. et al. (2017). "Forecasting consequences of changing sea ice availability for Pacific  
764 walruses". In: *Ecosphere* 8.11, e02014.

765 US Fish and Wildlife Service (2011). *Status review of the Pacific walrus (*Odobenus rosmarus divergens*)*.  
766 Tech. rep. U.S. Department of the Interior, U.S. Fish and Wildlife Service, Marine Mammals  
767 Management.

768 — (2023). *Pacific Walrus Stock Assessment Report 2023*. Tech. rep. U.S. Department of the Interior,  
769 U.S. Fish and Wildlife Service, Marine Mammals Management.

770 Wade, P. R. and D. P. DeMaster (1999). “Determining the optimum interval for abundance surveys”.

771 In: *Marine Mammal Survey and Assessment Methods*. CRC Press.

772 Waples, R. S. and P. Feutry (2022). “Close-kin methods to estimate census size and effective population

773 size”. In: *Fish and Fisheries* 23.2, pp. 273–293.

774 Williams, B. K., J. D. Nichols, and M. J. Conroy (2002). *Analysis and Management of Animal Popu-*

775 *lations*. Academic Press.

776 **Tables**

Table 1: Demographic parameters for simulation under four scenarios (D0, D1, D2, and D3). Scenario D0 was used to check the model code, whereas the other scenarios included reproductive senescence and were used to evaluate study design for a population that was either stationary (D1), decreasing (D2), or increasing (D3).

| Parameter   | Demographic Scenario |                  |                  |                  |
|---|----------------------|------------------|------------------|------------------|
|   | D0<br>NULL           | D1<br>Stationary | D2<br>Decreasing | D3<br>Increasing |
| Maximum age (AMAX)  | 37                   | 37               | 37               | 37               |
| Age at first birth for females (AFB)                      | 6                    | 6                | 6                | 6                |
| Age of last birth for females (ALB)                       | 37                   | 29               | 29               | 29               |
| Age of first fertility for males (AFF)                    | 15                   | 15               | 15               | 15               |
| Young-of-the-year (Age 0 calf) survival                   | 0.7                  | 0.7              | 0.66             | 0.7              |
| Juvenile survival (Ages 1 to 5)                           | 0.9                  | 0.9              | 0.85             | 0.925            |
| Reproductive adult female survival (Ages 6 to ALR)        | 0.9622               | 0.99             | 0.985            | 0.99             |
| Non-reproductive adult female survival (Ages ALR to AMAX) | NA                   | 0.55             | 0.5              | 0.55             |
| Probability of breeding at 2-yr interval ( $\psi_2$ )     | 0.1                  | 0.1              | 0.1              | 0.1              |
| Probability of breeding at 3-yr+ interval ( $\psi_3$ )    | 0.5                  | 0.5              | 0.5              | 0.5              |
| Resulting rate of increase ( $r$ )                        | 0                    | 0                | -0.02            | +0.01            |

Table 2: Details of sampling scenarios. For reference, scenarios are labelled S0-S8 with a description of effort. Effort per year is indicated as either 0, 0.75 (75%), or 1 (100%) effort as described in section 2.2. Each scenario was evaluated with and without the substitution of 500 lethal samples per year

| Sampling Scenario | Description                       | Effort per Year |      |      |      |      |      |
|-------------------|-----------------------------------|-----------------|------|------|------|------|------|
|                   |                                   | 2023            | 2024 | 2025 | 2026 | 2027 | 2028 |
| S0                | NULL: 100% effort 2023-2027       | 1               | 1    | 1    | 1    | 1    | 0    |
| S1                | Reality + 100% effort 2025        | 1               | 0    | 1    | 0    | 0    | 0    |
| S2                | Reality + 100% effort 2025-2026   | 1               | 0    | 1    | 1    | 0    | 0    |
| S3                | Reality + 100% effort 2025-2027   | 1               | 0    | 1    | 1    | 1    | 0    |
| S4                | Reality + 100% effort 2025-2028   | 1               | 0    | 1    | 1    | 1    | 1    |
| S5                | Reality + 75% effort 2025         | 1               | 0    | 0.75 | 0    | 0    | 0    |
| S6                | Reality + 75% effort 2025-2026    | 1               | 0    | 0.75 | 0.75 | 0    | 0    |
| S7                | Reality + 75% effort through 2027 | 1               | 0    | 0.75 | 0.75 | 0.75 | 0    |
| S8                | Reality + 75% effort through 2028 | 1               | 0    | 0.75 | 0.75 | 0.75 | 0.75 |

## 777 Figure Captions

778 Figure 1: Directed cyclic graph showing the breeding cycle for walruses as represented in our Markov  
779 model. Nodes show the states (pregnant, with young-of-the-year (YOTY), or quiescent) and edges  
780 give transition probabilities between those states. On average, female walruses reach sexual maturity  
781 (age of first ovulation) at age 4, so females enter the graph at the quiescent node. On the right is  
782 the transition matrix,  $\Psi$ , where cells indicate transition probabilities from row state to column state.

783 Figure 2: Expected CV of adult female abundance (vertical axis) in different years (horizontal axis)  
784 under different sampling scenarios (panel columns) for a simulated stationary population. For clarity,  
785 points have been jittered horizontally. Triangular points represent expected CVs from IMR alone,  
786 while circular points show expected CVs with ICKMR. The inclusion of lethal samples is indicated by  
787 filled (lethal samples substituted) or open (no lethal samples) points. The grey horizontal dot-dashed,  
788 dashed, and dotted lines at  $CV = 0.2, 0.1$ , and  $0.05$  respectively represent decision-making thresholds.

789 Figure 3: Total survey effort between 2023 and 2028 (in number of years, which may be a combination  
790 of calendar years of effort and fractional effort per year, horizontal axis) versus expected CV for adult  
791 female abundance in 2025 with IMR (triangular points) or with ICKMR (circular points) and with  
792 (filled) and without (open) the substitution of lethal samples for a simulated stationary population.  
793 The horizontal dot-dashed, dashed, and dotted lines at  $CV = 0.2, 0.1$ , and  $0.05$  respectively represent  
794 decision-making thresholds.

795 **Figures**

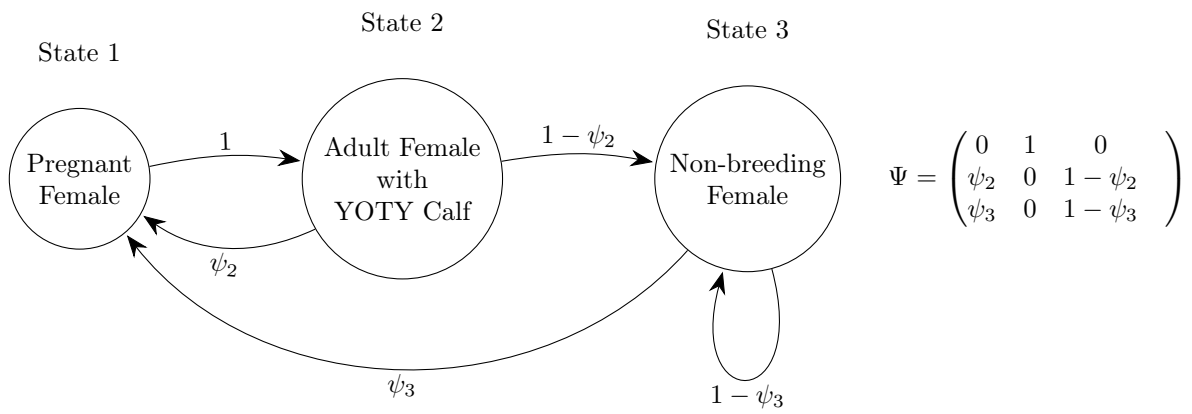


Figure 1:

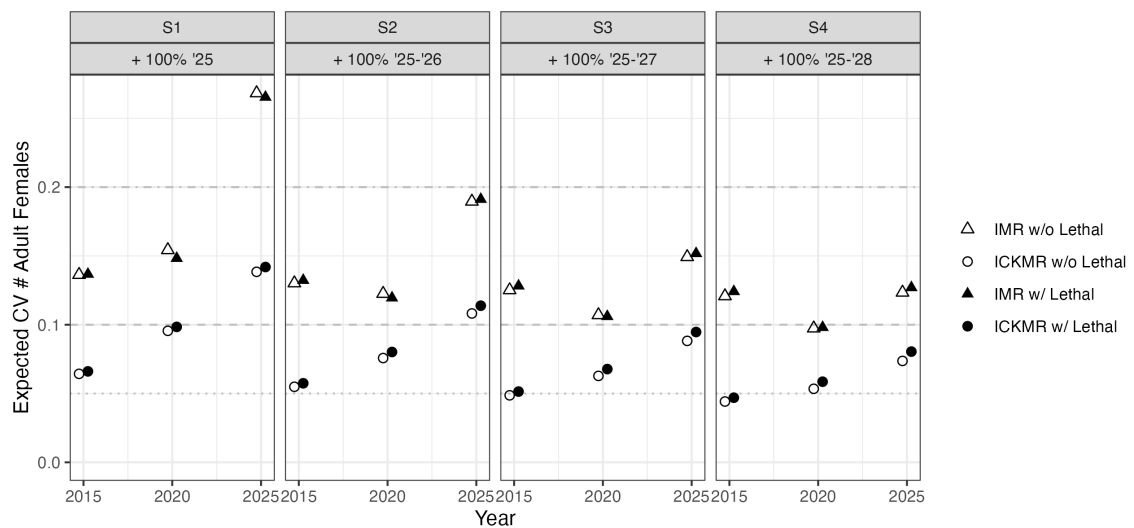


Figure 2:

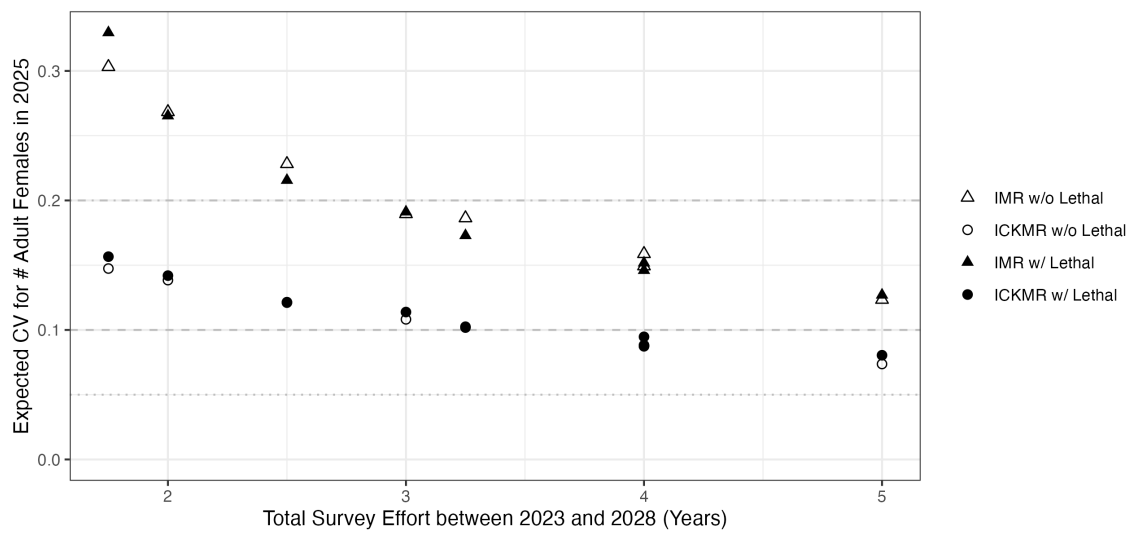


Figure 3: